

The holocentric species *Luzula elegans* shows interplay between centromere and large-scale genome organization

Stefan Heckmann¹, Jiri Macas², Katrin Kumke¹, Jörg Fuchs¹, Veit Schubert¹, Lu Ma¹, Petr Novák², Pavel Neumann², Stefan Taudien³, Matthias Platzer³ and Andreas Houben^{1,*}

¹Leibniz Institute of Plant Genetics and Crop Plant Research (IPK), Corrensstraße 3, 06466 Gatersleben, Germany,

²Biology Centre of the Academy of Sciences of the Czech Republic, Institute of Plant Molecular Biology, Branišovská 31, České Budějovice 37005, Czech Republic, and

³Leibniz Institute for Age Research – Fritz Lipmann Institute, Beutenbergstraße 11, 07745 Jena, Germany

Received 28 August 2012; revised 11 October 2012; accepted 16 October 2012; published online 12 December 2012.

*For correspondence (e-mail houben@ipk-gatersleben.de).

SUMMARY

In higher plants, the large-scale structure of monocentric chromosomes consists of distinguishable eu- and heterochromatic regions, the proportions and organization of which depend on a species' genome size. To determine whether the same interplay is maintained for holocentric chromosomes, we investigated the distribution of repetitive sequences and epigenetic marks in the woodrush *Luzula elegans* (3.81 Gbp/1C). Sixty-one per cent of the *L. elegans* genome is characterized by highly repetitive DNA, with over 30 distinct sequence families encoding an exceptionally high diversity of satellite repeats. Over 33% of the genome is composed of the Angela clade of Ty1/copia LTR retrotransposons, which are uniformly dispersed along the chromosomes, while the satellite repeats occur as bands whose distribution appears to be biased towards the chromosome termini. No satellite showed an almost chromosome-wide distribution pattern as expected for a holocentric chromosome and no typical centromere-associated LTR retrotransposons were found either. No distinguishable large-scale patterns of eu- and heterochromatin-typical epigenetic marks or early/late DNA replicating domains were found along mitotic chromosomes, although super-high-resolution light microscopy revealed distinguishable interspersed units of various chromatin types. Our data suggest a correlation between the centromere and overall genome organization in species with holocentric chromosomes.

Keywords: holocentric genome organization, holokinetic chromosome, centromere, histone marks, repetitive DNA, *Luzula elegans*.

INTRODUCTION

Most studied organisms feature one single size-restricted centromere per chromosome (monocentric chromosomes), but in certain independent eukaryotic lineages, holocentric chromosomes occur (Melters *et al.*, 2012). These holocentric chromosomes lack a primary constriction, and, in contrast to monocentric chromosomes, they form holokinetic kinetochores (also called diffuse or non-localized kinetochores) that are distributed along almost the entire poleward surface of the chromatids, to which the spindle fibers attach (Guerra *et al.*, 2010; Heckmann and Houben, 2012).

Centromere functions are highly conserved between mono- and holocentric chromosome species, and similar kinetochore components have been found in the active centromeres of both types (Maddox *et al.*, 2004; Nagaki *et al.*, 2005; d'Alençon *et al.*, 2011). However, structural analysis of mitotic chromosomes in the holocentric plant

genus *Luzula* challenged the notion of a 'diffuse' centromere organization along holocentric chromosomes (Nagaki *et al.*, 2005; Heckmann *et al.*, 2011). Instead, a longitudinal centromere-like groove that was positive for CENH3 [a mark for active centromeres (Kalitsis and Choo, 2012)] was found along each sister chromatid, discontinued at each sub-terminal end. Consistently, entire mitotic chromosomes of *Luzula* (Gernand *et al.*, 2003; Nagaki *et al.*, 2005) and *Rhynchospora tenuis* (Guerra *et al.*, 2006) displayed a cell cycle-dependent uniform histone H3S10/S28 phosphorylation mark, illustrating a chromosome-wide 'pericentromeric-like' structure (Houben *et al.*, 2007a).

The DNA of centromeres is highly variable, and, except for budding yeast (Clarke and Carbon, 1985), the sequences are neither necessary nor sufficient for centromere formation. However, satellite DNA repeats and

specific families of long terminal repeat (LTR) retrotransposons are usually associated with centromeres in monocentric plant species (Houben and Schubert, 2003; Neumann *et al.*, 2011). In contrast, for holocentric species, centromere-specific DNA sequences have not yet been reported (Gassmann *et al.*, 2012).

In addition to centromeres, heterochromatin-forming repeats are typically found at telomeres, nucleolar organizing regions, sub-terminal and interstitial regions in monocentric species (Schmidt and Heslop-Harrison, 1998). The genome organization is reflected by the distribution of epigenetic marks, such as DNA methylation and post-translational histone modifications. Typically, methylation of lysine residues 9 and 27 of histone H3 corresponds to heterochromatin, while euchromatin is marked by methylation of lysine residues 4 and 36 of histone H3 (Fuchs *et al.*, 2006). In most monocentric species with small genomes (1C < 500 Mbp), e.g. *Arabidopsis*, strong dimethylation of H3K9 is primarily limited to pericentromeric heterochromatin, while larger genome species show a uniform H3K9me2 distribution. In contrast, dimethylation of H3K4 is exclusively enriched at euchromatic regions along chromosome arms in monocentric species, regardless of their genome size. This observation suggests that genome size in monocentric species is a factor that significantly influences the global distribution of histone methylation marks at transcriptionally less active regions (Houben *et al.*, 2003; Fuchs *et al.*, 2006). However, studies on the chromosomal distribution of typical euchromatin and heterochromatin histone marks are lacking in holocentric plants.

In terms of the inter-relationship between centromere organization and chromosome structure, we wished to determine whether the higher-order composition of a holocentric chromosome displays the same characteristics as a monocentric one, and to address this question, we selected the woodrush *Luzula elegans* Lowe (formerly *L. purpurea*) as a model species, due to the low number and large size of its holocentric chromosomes (Heckmann *et al.*, 2011). Illumina sequencing, combined with bioinformatic and cytogenetic approaches, revealed a unique genome organization. In addition, an interspersed arrangement of eu- and heterochromatin marks, and of early and late replicating DNA, was found on the large scale. Our findings suggest interplay between the centromere and large-scale genome organization, and will therefore assist in the understanding of holocentric genome organization and its implications for genome evolution and centromere biology.

RESULTS

The repetitive DNA fraction of the *L. elegans* genome

The DNA content of nuclei was determined to be 7.80 pg per 2C using flow cytometry, corresponding to a

1C genome size of 3.81 Gbp, which is in close agreement with the measurements of Barlow and Nevin (1976). To obtain insight into sequence composition of repetitive sequences in this relatively large genome, high-throughput shotgun sequencing was performed on the Illumina GAIIx platform. The original Illumina sequencing data are available under study accession number ERP001569 (<http://www.ebi.ac.uk/ena/data/view/ERP001569>) at the Sequence Read Archive (<http://www.ebi.ac.uk/ena/>). A randomly sampled proportion (1.5 million) of generated reads was then subjected to bioinformatic analysis, implemented within the clustering-based repeat identification pipeline (Novak *et al.*, 2010). This analysis resulted in thousands of clusters, or groups of reads, with overlapping sequences, each representing a single repeated element or part of it. Following repeat classification within major clusters, the global repeat composition of the genome was determined by taking into account the sizes (number of reads) of individual clusters, which are proportional to the genomic abundance of corresponding repeats. The *L. elegans* genome was found to be rich in repeated sequences, with highly and moderately repeated elements represented by clusters with genome proportions of at least 0.01% and collectively making up 61% of the genome. The majority of these sequences were classified into established groups of repetitive elements, revealing the Angela clade of Ty1/copia LTR retrotransposons to be a dominant repeat representing over 33% of the genome (Table 1). Except for the satellite repeats, the proportions of all other repeat types, including various groups of LTR retrotransposons, did not exceed a few per cent of the genome. Some repeats were completely absent, including the CRM clade of Ty3/gypsy retrotransposons that are known to be specifically associated with plant centromeres (Neumann *et al.*, 2011). The observed proportion of plastid DNA reads (3.4%) most likely originated from contamination of nuclear DNA preparations by the chloroplast genome, because no signals were detectable on chromosomes by fluorescence *in situ* hybridization (FISH) using plastid DNA as a probe (data not shown), although we cannot rule out the possibility of low-copy insertions of plastid DNA into the nuclear genome.

Table 1 Repetitive DNA composition of the *L. elegans* genome

Type of repeat	Proportion of the genome (%)
Ty1/copia, Angela clade	33.4
Ty1/copia, Maximus clade	0.9
Ty3/gypsy	1.1
LTR unclassified	2.0
Long interspersed elements (LINEs)	0.3
DNA transposons	1.1
rDNA	0.3
Satellites	9.9

Although the overall genome proportion of satellite DNA was not exceptional compared to other plant species, there was an extraordinary sequence diversity of tandem repeats found in the *L. elegans* genome. Thirty-seven families of putative satellite repeats differing in their monomer lengths and sequence composition were identified among 291 major repeat clusters (genome proportions of at least 0.01%). The characteristics of the 20 largest satellite DNA clusters are provided in Table 2, and their dot-plot sequence comparison is shown in Figure S1 (assembled contigs representative for each cluster are listed in Data S1). Although some of the identified families had monomer sizes in the range of hundreds of nucleotides, which is typical for the majority of known plant satellites (Macas *et al.*, 2002), 12 of the 20 families had shorter monomer sequences, ranging from 90 bp down to the size of micro-satellite repeats (Table 2). The tandem genomic organization of some of the identified satellite repeats was verified by Southern hybridization to partially digested genomic DNA, revealing typical ladder-like hybridization patterns as demonstrated for LeSAT4, LeSAT11 and LeSAT9 + 21 (Figure S2).

Satellite repeats tend to localize at chromosome termini

Fluorescence *in situ* hybridization probes (Table S1) derived from conserved regions of the 20 selected satellite repeats (Table 2) were used to investigate their distribution on mitotic chromosomes. All of them provided signal patterns consisting of multiple discrete bands, or spots,

that are typical of satellite repeats organized in long monomer arrays. Most satellites were detected on all three pairs of chromosomes; although chromosome-specific families were also observed labeling two chromosome pairs (LeSAT23, 25, 27, 28, 36 and 99), or one chromosome pair only (LeSAT43 and 63). There were also families that labeled particular chromosome regions, i.e. LeSAT7, 11 and 109, which labeled the terminal regions, and LeSAT4, which clustered on each chromosome at almost symmetrical distal positions. As all chromosomes are equally sized, and are not distinguishable by their morphology, two probes, LeSAT28 and LeSAT63, were combined to provide a hybridization pattern facilitating their discrimination. LeSAT28-specific signals occurred distally on chromosome 1, opposite the 45S rDNA locus, and (sub)terminally on chromosome 2 (Figure 1a). LeSAT63 localized interstitially on chromosome 2, being slightly more distal towards the LeSAT28-bearing chromosome region (Figure 1a). Although the minor LeSAT28 signal on chromosome 2 was not always detectable, the combination of LeSAT28 and 63 allowed discrimination of all chromosomes. The resulting karyogram based on these probes is shown in Figure 1(b).

None of the tested satellite repeats displayed a distribution pattern expected for the almost chromosome-wide distribution of the centromere in *Luzula* (Figure 1 and Figure S3). Instead, we noticed a tendency for distal satellite clustering, especially at the centromere-free chromosome termini. To confirm this observation, distinct FISH signals of all satellites were classified into centromeric and

Table 2 Characteristics of the most abundant satellite repeats in the *L. elegans* genome

Satellite	Cluster	Cluster size (reads)	Genome proportion (%)	Monomer (bp)	Notes
LeSAT4	4	33.681	2.25	190/220/360	Several closely related sequence variants differing in monomer length
LeSAT7	7	17.900	1.19	75	
LeSAT9 + 21	9 + 21	21.068	1.40	43	LeSAT9 and LeSAT21 contain two highly similar sub-families of the same satellite
LeSAT11	11	13.038	0.87	56	
LeSAT16	16	7495	0.50	178/195/...	Heterogeneous repeat, contains several sub-families differing in monomer size
LeSAT17	17	7210	0.48	161	
LeSAT18	18	6156	0.41	Variable	Non-homogenized tandem repeat, contains tandem sub-repeats of various lengths (tens of bp)
LeSAT22	22	5262	0.35	51/167	
LeSAT23	23	4721	0.31	57	
LeSAT25	25	4084	0.27	6	Simple sequence repeat (CATAAA) _n
LeSAT27	27	3946	0.26	42	
LeSAT28	28	3815	0.25	390/730	
LeSAT36	36	3031	0.20	6	Simple sequence repeat (CATAAC) _n
LeSAT38	38	2846	0.19	137	
LeSAT43	43	2494	0.17	190	
LeSAT63	63	1433	0.10	90	
LeSAT72	72	1192	0.08	4	Simple sequence repeat (CATA) _n
LeSAT89	89	945	0.06	41	
LeSAT99	99	816	0.05	180	
LeSAT109	109	710	0.05	33	Partial similarity to LeSAT99

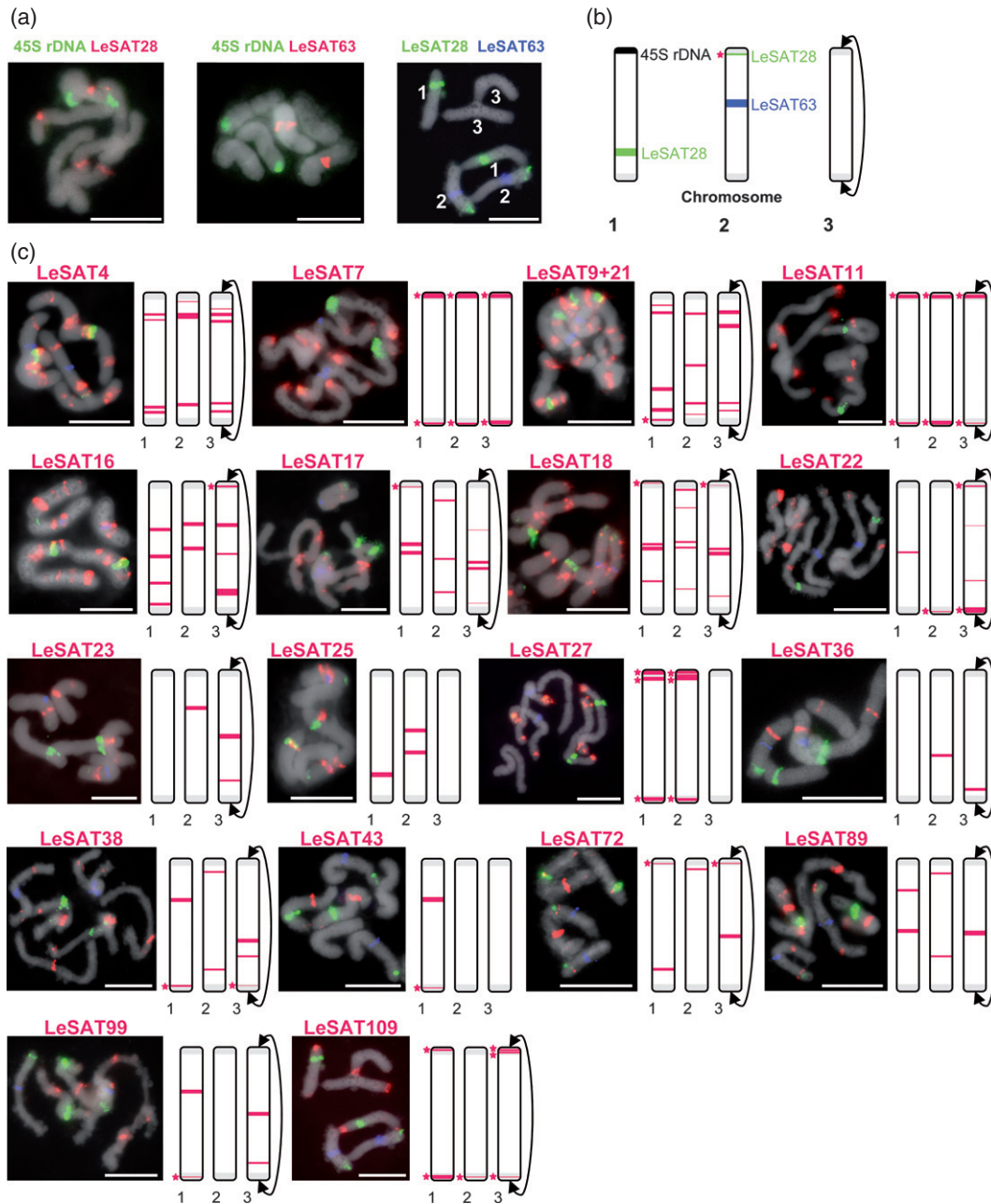


Figure 1. Distribution of satellite DNA on *L. elegans* mitotic metaphase chromosomes studied by FISH. (a) LeSAT28 and LeSAT63 (red) localized individually in relation to a 45S rDNA probe (green), and relative to each other (green, LeSAT28; blue, LeSAT63). (b) Karyogram based on probes used in (a), allowing discrimination of the three equally sized chromosomes. (c) FISH experiments with various LeSATs (pink) together with LeSAT28 (green) and LeSAT63 (blue), and the resulting schematic ideograms. DAPI-stained DNA is shown in gray. The gray-shaded chromosome ends in schematic ideograms represent defined terminal (non-centromeric) chromosome regions accounting for approximately 10% of the total chromosome size. Asterisks indicate FISH signals counted as terminal (non-centromeric) satellite clusters (see Table 3). Scale bar = 10 μm.

non-centromeric clusters (Table 3). To ensure a clear distinction between centromeric and non-centromeric chromosome regions, only clusters within the terminal 5% of chromosome ends were counted as non-centromeric regions, i.e. both terminal regions correspond to approximately 10% of the total chromosome length. Note, the centromere discontinues at each sub-terminal chromosome

end and represents on average 75% of metaphase chromosome length as shown by CENH3-immunolabeling and scanning electron microscopy, respectively (Figure S3; Heckmann *et al.*, 2011). Thus, the percentage of non-centromeric clusters may be under-estimated. Of the 122 identified clusters of satellites, 39 (approximately 32%) localized to terminal non-centromeric chromosome

Table 3 Satellites are proportionally more frequent in non-centromeric than in centromeric chromosomal regions

	Chromosome 1	Chromosome 2	Chromosome 3	All chromosomes
Number of clusters	42	37	43	122
Number of centromeric clusters (%)	26 (61.9)	27 (73)	30 (69.8)	83 (68)
Number of non-centromeric cluster (%)	16 (38.1)	10 (27)	13 (30.2)	39 (32)
Ratio of relative cluster abundance in non-centromeric versus centromeric regions ^a	5.5:1	3.3:1	3.9:1	4.2:1

FISH signals of all studied satellites are classified into centromeric and non-centromeric clusters (see Figure 1). Their abundance per chromosome is given. Defined centromeric and non-centromeric chromosome parts represent approximately 90% and 10% of the total chromosome length, respectively (see Figure 1).

^aThe relative cluster abundance is calculated based on the absolute values of satellite clusters in non-centromeric and centromeric regions given their different lengths.

regions, while 83 (approximately 68%) localized to interstitial centromeric regions (Table 3). The amount of non-centromeric clusters varied between chromosomes, i.e. from approximately 27% on chromosome 2 to approximately 38% on chromosome 1 (Table 3). As the terminal non-centromeric regions represent only approximately 10% of the total chromosome length, the abundance of satellite clusters in these regions is on average 4.2-fold higher than in interstitial centromeric regions.

In contrast to the satellite repeats, the probes derived from mobile elements showed uniformly dispersed chromosome patterns (Figure 2). The probes were either prepared from shotgun-cloned *L. elegans* genomic fragments, corresponding to partial sequences of the Ty1/copia element Angela (Table S2), or from PCR products using primers based on the contig CL8c28 (assembled contigs are listed in Data S1) corresponding to LTR and gag-pol regions of elements from the chromovirus clade of

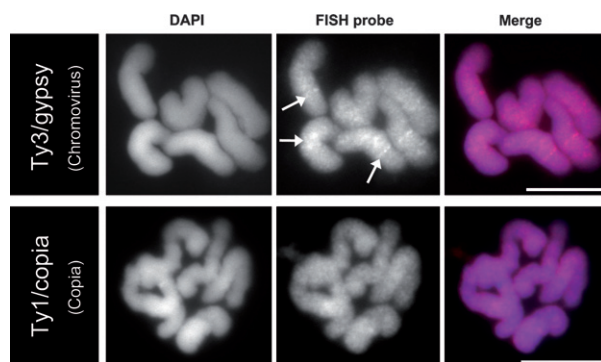


Figure 2. Distribution of LTR retrotransposons on *L. elegans* mitotic chromosomes.

Probes were derived from sequences of Angela-like elements and chromoviruses, representing the most abundant clades of Ty1/copia and Ty3/gypsy elements in the *L. elegans* genome, respectively. Note some interstitial centromere-atypical clustering of Ty3/gypsy elements indicated by arrows. Two Ty3/gypsy-specific probes representing either the gag-pol (CL8c28_1) or LTR (CL8c28_2) regions showed similar patterns. CL8c28_1 (see Table S1) and clone 5 (see Table S2) are shown as Ty3/gypsy- and Angela-specific probes, respectively. In the merged image, DAPI-stained DNA is shown in blue and LTR retrotransposons appear red. Scale bar = 10 μm.

Ty3/gypsy retrotransposons (Table S1). A clone containing an abundant microsatellite motif [(TA)_n] generated a similar pattern (Table S2).

Uniformly mixed genome organization of *Luzula* on a large scale, with defined subunits at a lower chromatin organization level

To examine whether the genome of *L. elegans* is organized on a large scale into eu- and heterochromatin-enriched sub-regions, we used antibodies against typical euchromatin- and heterochromatin-specific histone marks. In contrast to previous reports for monocentric species (Houben *et al.*, 2003), immunostaining with a euchromatin-specific antibody such as H3K4me2 revealed uniform labeling of the entire chromosome and interphase nuclei (Figure 3).

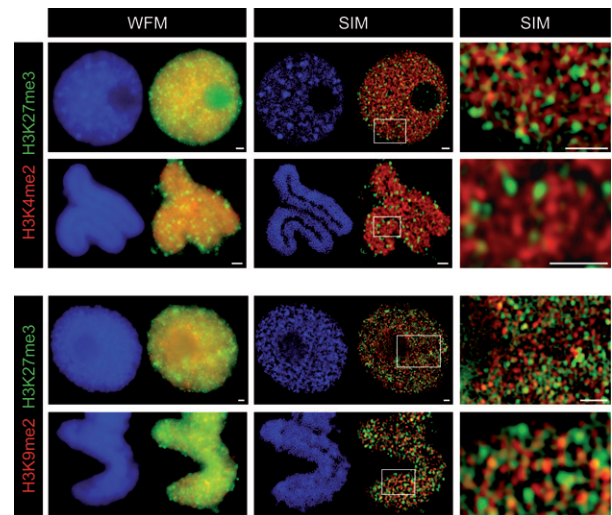


Figure 3. Distribution of histone H3K4me2, H3K9me2 and H3K27me3 in *L. elegans*.

Double immunolabeling with H3K4me2 and H3K27me3, as well as with H3K9me2 and H3K27me3, for interphase nuclei and mitotic chromosomes. High-resolution imaging by structured illumination microscopy (SIM, centre and right) compared to normal fluorescence wide-field microscopy (WFM, left). Enlargements of the regions delimited by the white boxes are shown. DNA appears blue and histone marks appear red and green. Scale bar = 1 μm.

A comparable distribution was found for the heterochromatin marks H3K9me2 and H3K27me3 (Figure 3), as well as for methylated DNA (Figure S4).

Next, immunolabeled cells were analyzed by structured illumination microscopy (SIM) to obtain a higher optical resolution of eu- and heterochromatin-specific immunosignals at approximately 100 nm. Various sub-domains were detected: hetero- or euchromatin-containing domains and intermingled eu- and heterochromatin domains (Figure 3). The two heterochromatin marks H3K9me2 and H3K27me3 also revealed a subunit organization into chromatin units that shared both marks, or were free of one or the other or both marks (Figure 3). Interphase nuclei showed either uniform chromatin or DAPI-enriched 'chromocenters', most likely based on the cell cycle or cell type. However, at the chromosomal level, chromatin is mostly uniformly shuffled on a global view. Thus, *L. elegans* appears to represent an interspersed arrangement of euchromatic and heterochromatic domains on a large scale, while a distinct chromatin sub-organization into chromatin subunits is detectable using super-high-resolution light microscopy.

The DNA replication behavior was studied to test whether early- and late-replicating chromosome regions occupy distinct chromosomal regions, as in most monocentric species (Costas *et al.*, 2011). *Luzula* seedlings were therefore treated with 5-ethynyl-2'-deoxyuridine (EdU) for 5–135 min, and then seedlings were incubated in the absence of EdU so that the cells in S phase progressed to mitosis. The approximate time from S phase until entry into mitosis was estimated to be between 7.5 and 9 h, similar to other studies (Bernardini and Lima-de-Faria, 1967). Independently of the length of the EdU pulse, almost uniformly labeled chromosomes and nuclei were found (Figure 4 and Figure S5). Previous reports in *L. elegans* also described more or less randomly distributed DNA (late-) replicating sites along chromosomes (Bernardini and Lima-de-Faria, 1967; Ray and Venkateswaran, 1979). However, in the case of nuclei, a sub-fraction of 192 EdU-positive nuclei after a 5 min EdU pulse were found to be labeled with spots. A variable spotted pattern occurred in 29.8% of counted nuclei, while the remaining ones showed uniform labeling (Figure 4). Thus, it seems likely that replication clusters may occur, depending on the stage of the cell cycle or the cell type, as also indicated by the 'chromocenters' observed by SIM (Figure 3). However, a mostly dispersed and equally distributed replication pattern was observed for all chromosome pairs, and, on the large scale, the chromosomes of *L. elegans* are not compartmentalized into clearly distinguishable early- and late-replicating sub-regions. It is likely that early- and late-replicating sequences are equally distributed along the chromosomes. This result probably reflects the uniformly mixed genome organization, as also indicated by eu- and heterochromatin-specific marks.

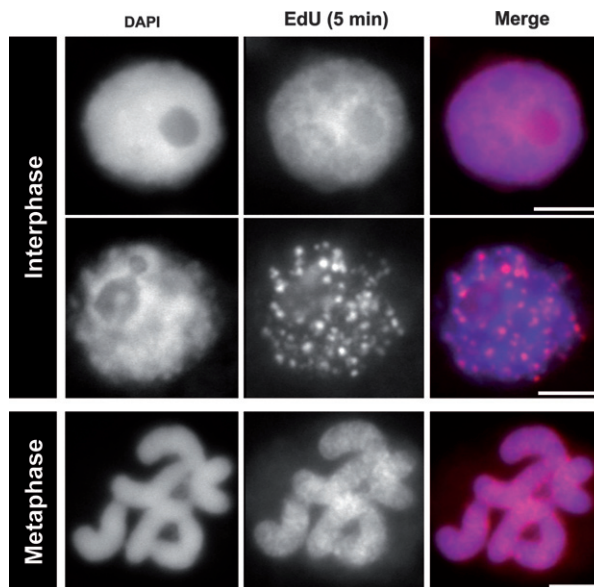


Figure 4. DNA replication behavior of *L. elegans*. Replication pattern of mitotic metaphase chromosomes and interphase nuclei after a 5 min EdU pulse followed by a 8.5 h H₂O incubation step.

Note, in the case of nuclei, two replication patterns were observed, with either uniform or spotted labeling, while chromosomes were uniformly labeled. In the merged image, DNA appears blue and EdU appears red. Scale bar = 5 μ m.

DISCUSSION

Do terminal satellites play a role in holocentric chromosome structure and function?

We performed a comprehensive characterization of the repetitive fraction of a holocentric plant genome. The content of highly repetitive DNA in *L. elegans* (61% of the 3.81 Gbp/1C-sized haploid genome) is in the same range as in monocentric plants with a comparable genome size that were analyzed with the same method [i.e. *Silene latifolia* males (2.93 Gbp/1C), 61.4%; females (2.87 Gbp/1C), 63.3% (Macas *et al.*, 2011), and *Pisum sativum* (4.3 Gbp/1C), 35–48% (Macas *et al.*, 2007)]. Holocentric species with smaller genomes contain less repetitive DNA, such as nematodes [i.e. *Caenorhabditis briggsae* (104 Mbp), 22.4%; *C. elegans* (100.3 Mbp), 16.5% (*C. elegans* Sequencing Consortium, 1998; Stein *et al.*, 2003)] and *Bombyx mori* [432 Mbp, 43.6% (Xia *et al.*, 2008)]. Thus, in holocentric species, the content of highly repetitive DNA is also greater in species with larger genomes.

Transposable elements largely account for genome size differences in plants (Hawkins *et al.*, 2006; Tenaillon *et al.*, 2011). In *L. elegans*, Ty1/copia elements are much more abundant than Ty3/gypsy elements, with the Angela clade elements the most abundant Ty1/copia element and constituting by far the most abundant repetitive fraction in the genome. *L. elegans* contains a rather large and heterogeneous fraction of satellites compared to plants with a

comparable genome size. In *S. latifolia*, only four families of satellite DNA were identified using the same *in silico* method (Macas *et al.*, 2011). It is likely that *L. elegans*-specific amplification of Ty1/copia elements from the Angela clade and of satellite repeats is the driving force behind the exceptionally large genome size of the genus *Luzula*. Other members of the genus are characterized by smaller genomes, ranging from 0.26 to 1.99 Gbp/1C (Bennett and Leitch, 2010).

The distal chromosome regions of *L. elegans* tend to be enriched in satellite DNA. Although some central blocks are found, the preferential localization of repetitive DNA and of heterochromatin in (sub)terminal regions seems to be a common feature of holocentric plants (Sheikh and Kondo, 1995; Vanzela and Guerra, 2000; Guerra and Garcia, 2004), and also of holocentric autosomes in animals (*C. elegans* Sequencing Consortium, 1998; Spence *et al.*, 1998; Tartarotti and de Azeredo-Oliveira, 1999; Mola and Papeschi, 2006; Hill *et al.*, 2009). In contrast, in many monocentric organisms, high-copy repeats and heterochromatin typically cluster at centromeres and various other sites (Schmidt and Heslop-Harrison, 1998; Mola and Papeschi, 2006; Lamb *et al.*, 2007). Surprisingly, in *L. elegans*, no correlation between enriched terminal satellites and epigenetic chromatin modifications was found, similar to *C. elegans*, in which heterochromatin is cytologically absent (Albertson *et al.*, 1997). It seems likely that, in these situations, enriched repressive domains are interspersed with active chromatin, and therefore no enrichment of heterochromatin-typical marks was detectable.

It is an obvious question whether a functional inter-relationship exists between terminally enriched satellite DNA and holocentricity. First, mutual exclusion of heterochromatin and centromere function may account for repetitive DNA accumulation in non-centromeric chromosome ends, as speculated for the nucleolar organizing region (Heckmann *et al.*, 2011). Secondly, in holocentric species, terminal heterochromatin may be involved in the physical end-to-end association of homologous chromosomes (rod bivalents) during meiotic divisions (Nordenskiöld, 1962; Dernburg, 2001; Bongiorno *et al.*, 2004; Guerra *et al.*, 2010; Heckmann and Houben, 2012).

Are there centromere-specific sequences in holocentric species?

The low abundance of Ty3/gypsy repeats and the absence of typical centromere-associated Ty3/gypsy retrotransposons of the CRM clade in *L. elegans* were surprising. Even an in-depth screen for low-copy chromodomain sequences of all available 21.4 million sequence reads revealed no significant hits for CRM elements, which typically colonize centromeric regions in monocentric plants (Neumann *et al.*, 2011). Moreover, none of the identified satellite repeats gave rise to a distribution pattern that was

expected for the almost chromosome-wide centromere distribution.

In *Luzula nivea*, a 178 bp tandem repeat sequence (LCS1; also present in nine other *Luzula* species) (Haizel *et al.*, 2005) sharing similarity with the centromeric tandem repeat RCS2 of rice (Dong *et al.*, 1998; Nonomura and Kurata, 2001) has been described. LCS1 clusters into tandem arrays of at least 50 kb at heterochromatic regions along each of the *L. nivea* chromosomes (Haizel *et al.*, 2005). Whether LCS1 plays a centromeric role is uncertain. Interestingly, no LCS1-related sequences were found in a BLAST similarity search of all available 21.4 million *L. elegans* sequence reads in this study.

Given the sequence-independent incorporation of CENH3 in *C. elegans* (Gassmann *et al.*, 2012), the sequence-independent formation of centromeres in nematodes (Howe *et al.*, 2001), and the absence of centromeric sequences even in the genome-sequenced holocentric animals *C. elegans* (*C. elegans* Sequencing Consortium, 1998; Gassmann *et al.*, 2012) and *B. mori* (Xia *et al.*, 2008; d'Alençon *et al.*, 2010), it is also likely that no typical centromeric sequences exist in *L. elegans*. More likely, a centromere-specific chromatin status exists that preferentially associates with CENH3 in *L. elegans*. Even in monocentric plants and animals, the occurrence of neocentromeres demonstrates that the centromeric DNA sequence itself is neither necessary nor sufficient to determine centromere function, and centromeres are determined epigenetically (Guerra *et al.*, 2010; Kalitsis and Choo, 2012).

Holocentric chromosomes: multiple sequence-independent centromeric subunits along chromosomes

A centromeric subunit organization as originally proposed by Zinkowski *et al.* (1991) for monocentric eukaryotes probably also applies for holocentric species, as *C. elegans* shows a centromeric subunit organization along holocentric chromosomes (Gassmann *et al.*, 2012) as well as *L. elegans*, as indicated by the mixed genome organization at the large scale, and the chromatin subunit organization at a higher resolution. A dispersed CENH3 distribution (dot-like foci) during interphase and prophase is found in *Luzula* (Nagaki *et al.*, 2005; Heckmann *et al.*, 2011) and *C. elegans* (Buchwitz *et al.*, 1999), indicating multiple centromeric subunits that fuse during metaphase to one functional kinetochore unit. Thus, holocentric chromosomes appear to be composed of multiple centromere units interspersed by non-centromeric chromatin all along their length (Figure 5).

Neumann *et al.* (2012) showed that the tandem organization of multiple satellites, but not their primary sequence, determines the presence of remarkably large functional centromeres in pea that are 'intermediate between monocentric and polycentric'. Unlike most other monocentric species (Hall *et al.*, 2004), the centromeric DNA sequence

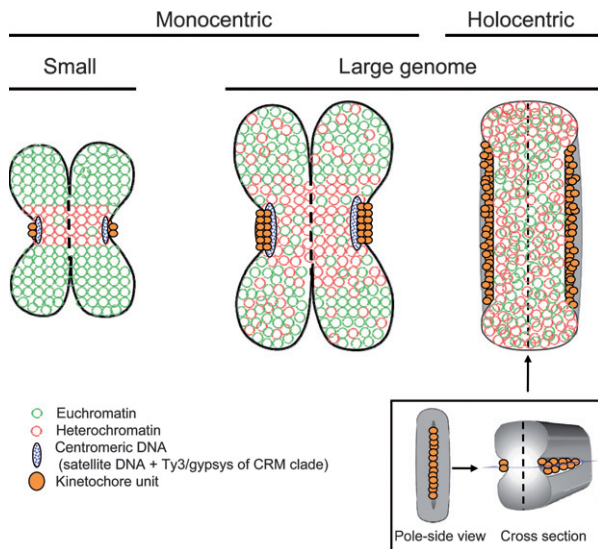


Figure 5. Schematic model of the distribution of eu- and heterochromatin as well as of the centromere in holocentric versus monocentric chromosomes, according to genome size.

In monocentric species, chromosomes are sub-structured into distinguishable eu- and heterochromatic regions according to genome size. Typically, monocentric centromeres are colonized by satellite DNA repeats and specific LTR retrotransposons (Ty3/gypsy of the CRM clade). In small genome species ($1C < 500$ Mbp), H3K9me2 is concentrated within cytologically defined heterochromatin, while large-genome ($1C > 500$ Mbp) species show a uniform distribution of H3K9me2. However, dimethylated H3K4 is enriched within the euchromatin of all monocentric species, regardless of genome size. In contrast, in holocentric chromosomes, an inter-mixed arrangement of eu- and heterochromatin exists. DNA sequence-independent centromere units are interspersed by non-centromeric chromatin all along their length. Centromeric units fuse during metaphase to one functional kinetochore unit, leading to formation of a centromeric groove in holocentric species such as *L. elegans*. Only chromosome termini tend to be enriched in heterochromatin.

composition is highly variable in pea. Thirteen of 19 distinct satellite families, and one family of Ty3/gypsy retrotransposons of the CRM clade, are centromere-associated (Neumann *et al.*, 2012). Thus, pea is the most similar studied organism so far with respect to the number and diversity of satellites. It is tempting to speculate that the larger a centromere gets, the more important the centromere-specific chromatin status or organization becomes, and the less important the primary DNA sequence is. Even in holocentric organisms, there are apparently multiple sequence-independent centromeric subunits along the chromosomes (Gassmann *et al.*, 2012). However, dicentric chromosomes break during anaphase when they reach a critical distance between both active centromeres, thus not forming one functional kinetochore during metaphase (Higgins *et al.*, 2005; Zhang *et al.*, 2010). The distance between individual kinetochore subunits in holocentrics must therefore be restricted. However, it is not known what the minimal distance between individual kinetochore subunits is for formation of a composite linear-like kinetochore.

Is there interplay between centromere and large-scale genome organization?

Early reports in *L. elegans* described more or less evenly distributed heterochromatin, by C-banding, with a slight tendency for interstitial and terminal heterochromatin clusters and multiple randomly distributed DNA (late-) replicating sites (Bernardini and Lima-de-Faria, 1967; Ray and Venkateswaran, 1978, 1979). We found an overlap of eu- and heterochromatin-specific histone marks, homogeneously dispersed DNA methylation and mobile elements along chromosomes on a global view, as well as equally distributed early- and late-replicating sequences all along *L. elegans* chromosomes. Other *Luzula* species are also characterized by dispersed heterochromatin and repetitive DNA along chromosomes (Collet and Westerman, 1984, 1987). Studies in *Luzula flaccida* (Collet and Westerman, 1984) and holocentric animals (Albertson *et al.*, 1997; d'Alençon *et al.*, 2010; Liu *et al.*, 2011) also indicate an interspersed arrangement of eu- and heterochromatic domains along chromosomes.

The almost chromosome-wide distribution of the centromere into multiple centromeric subunits is the most likely reason why holocentric species are characterized by an inter-mixed arrangement and homogenization of chromatin states throughout their genomes. Thus, it is plausible to speculate that the large-scale genome organization differs between monocentric and holocentric species (Figure 5), although further studies in holocentric species are required to verify this hypothesis.

EXPERIMENTAL PROCEDURES

Plant material and culture conditions

Luzula elegans ($2n = 6$) plants (Vouchers at the Herbarium Gatersleben; GAT 7852-7856) were germinated in Petri dishes on wet filter papers under long-day conditions (16 h light/8 h dark, $20^{\circ}\text{C}/18^{\circ}\text{C}$), transferred to soil, cultivated for 6–8 weeks under short-day conditions (8 h light/16 h dark, $20^{\circ}\text{C}/18^{\circ}\text{C}$), transferred to vernalizing conditions (10 h light/14 h dark, 4°C), and finally returned to long-day conditions (13 h light/11 h dark, $20^{\circ}\text{C}/16^{\circ}\text{C}$).

Genomic DNA isolation, Southern and dot-blot hybridization

Genomic DNA was isolated using a DNeasy plant maxi kit (Qiagen, <http://www.qiagen.com>), according to the manufacturer's instructions, and, if required, digested using *Bam*HI, *Eco*RI, *Hpa*II or *Msp*I, electrophoresed in a 0.8% w/v agarose gel and transferred by alkaline transfer to Hybond N+ membranes. Southern and dot-blot hybridization were performed as described by Houben *et al.* (1996). The membranes were probed with ^{32}P -labeled DNA probes.

Illumina sequencing

The genomic DNA was fragmented by nebulization, and a paired-end library with fragment lengths of approximately 500 bp was prepared according to the manufacturer's instructions (Illumina, <http://www.illumina.com>). Sequencing was performed on one lane

of an Illumina Genome Analyzer IIx system using Illumina's paired-end cluster generation and cycle sequencing kits.

Repeat identification and characterization

Identification of repetitive sequences was achieved using similarity-based clustering analysis of sequence reads as described by Novak *et al.* (2010). The analysis was performed using a set of 1.5 million reads randomly selected from a total of 21.4 million high-quality Illumina forward sequence reads. A similarity cut-off of 90% over at least 80% of the read length was used for the clustering, and the reads within individual clusters were assembled and further investigated using a set of custom-written BioPerl and R scripts to determine which type and family of repeats they represent (Macas *et al.*, 2007; Novak *et al.*, 2010). Clusters containing satellite repeats were identified based on the presence of tandem sub-repeats within their read or assembled contig sequences. These satellite repeats were characterized using oligomer frequency analysis of the reads within their clusters as described previously (Macas *et al.*, 2010).

Plasmid library construction and dot blotting

Genomic DNA was fragmented by sonication. Jagged ends were removed using BAL-31 exonuclease (New England BioLabs, <http://www.neb.com>). DNA was purified and electrophoresed in a 1% w/v agarose gel. A 150–600 bp fraction was excised, and the ends were repaired by T4 DNA polymerase and Klenow fragment activity. Repaired fragments were A-tailed by Taq polymerase treatment and cloned into the pCR[®]2.1 vector (Invitrogen, <http://www.invitrogen.com>). Dot blotting was performed as described by Houben *et al.* (1996). Plasmid DNA (2 µg) was dot-blotted onto membranes by the alkaline method and hybridized to ³²P-labeled genomic DNA.

Flow cytometric genome size measurement

Genome size was estimated as described previously (Fuchs *et al.*, 2008) using *Pisum sativum* cv. 'Viktoria, Kifejtö Borsó' (Genebank Gatersleben accession number PIS 630; 2C = 9.09 pg) (Doležel *et al.*, 1998), as an internal reference standard. In total, 21 individuals were measured, divided into three independent experiments performed on different days.

Indirect immunolabeling

Apical meristems of young plants were fixed for 45 min in ice-cold 4% w/v paraformaldehyde in PBS. After washing 3 times for 10 min in ice-cold PBS, chromosome spreads were prepared by squashing. Immunolabeling was performed as previously described (Houben *et al.*, 2007b). The following dilutions of primary antibodies were used: 1:200 for a rabbit anti-H3K4me2 antibody (Millipore, <http://www.millipore.com>), 1:200 for a rabbit anti-H3K9me2 antibody (Active Motif, <http://www.activemotif.com>), 1:50 for a mouse anti-H3K27me3 antibody (Abcam, <http://www.abcam.com>) and 1:100 for a rabbit anti-LnCENH3 antibody (Nagaki *et al.*, 2005). Immunodetection using 5-methylcytosine (1:300 dilution) (Eurogentec, <http://www.eurogentec.com>) was performed as described by Marques *et al.* (2011). A Cy3-conjugated anti-rabbit IgG (Dianova, <http://www.dianova.com>) and a fluorescein isothiocyanate-conjugated anti-mouse Alexa 488 antibody (Molecular Probes, <http://www.invitrogen.com>), each at 1:400 dilution, were used as secondary antibodies. Fluorescence images were recorded using an Olympus BX61 microscope (Olympus, <http://www.olympus.com>) equipped with an ORCA-ER CCD camera (Hamamatsu, <http://www.hamamatsu.com>). 3D deconvolution microscopy was used to

reduce out-of-focus information for globular structures. Image stacks of 10–11 slices per specimen were acquired, and the maximum-intensity projections were processed using the program AnalySIS (Soft Imaging System, <http://www.soft-imaging.net>). Grey-scale images were pseudocolored using Adobe Photoshop (<http://www.adobe.com>). To achieve an optical resolution of approximately 100 nm, structured illumination microscopy (SIM) was applied using a C-Apo 63×/1.2 W Korr objective with an Elyra microscope system (Zeiss, <http://www.zeiss.com>).

Probe preparation and fluorescence *in situ* hybridization

FISH probes were obtained as 5'-Cy3, 5'-Cy5- or 5'-Alexa 488-labeled oligonucleotides (Eurofins MWG Operon, <http://www.eurofinsdna.com>), or were PCR-amplified. The sequences of all oligonucleotides are listed in Table S1. Nuclear ribosomal 45S rDNA was probed using the clone pTa71 (Gerlach and Bedbrook, 1979), and plastid DNA was probed using the clone HVVMRXALLhC0205G01 (Schulte *et al.*, 2011), respectively. All DNA probes, except oligonucleotides, were labeled with Texas Red-, Cy5- or Alexa 488-dUTP by nick translation as described by Kato *et al.* (2006).

Chromosome spreads were prepared from apical meristems fixed using 3:1 v/v ethanol/acetic acid. Specimens were dehydrated in an ethanol series, air-dried, and cross-linked using an UV-light illuminator (0.12 J cm⁻²) (Biometra, <http://www.biometra.com>). Probe(s) were then mixed with the hybridization mixture (50% formamide and 20% dextran sulfate in 2× SSC), dropped onto slides, covered with a cover slip, and sealed using 'fixogum' (Marabu, <http://marabu-kreativ.de>). After denaturation on a heating plate at 80°C for 3 min, slides were hybridized at 37°C overnight. Post-hybridization washing was performed in 2× SSC for 20 min at 58°C. After dehydration in an ethanol series, 4',6'-diamidino-2-phenylindole (DAPI) in Vectashield (Vector Laboratories, <http://www.vectorlabs.com>) was applied. Fluorescence images were obtained as described above.

DNA replication analysis

Eighteen-day-old seedlings were incubated in 20 µM 5-ethynyl-2'-deoxyuridine (EdU) in H₂O for varying times, followed by multiple washing steps in H₂O allowing EdU-incorporated cells to enter mitosis, and then fixed in 3:1 v/v ethanol/acetic acid overnight. Slides were prepared as described above for apical meristems. EdU incorporation was detected by the click reaction, using the Click.iT EdU Imaging Kit (Invitrogen). After washing in 2× SSC, DAPI in Vectashield (Vector Laboratories) was applied. Fluorescence images were obtained as described above.

ACKNOWLEDGEMENTS

We are grateful to Oda Weiß, Marlene Zimmer and Susann Schier (IPK, Department Cytogenetics and Genome Analysis, Gatersleben) for their excellent technical assistance. We also thank Maria Cuacos (Departamento de Genética, Facultad de Biología, Universidad Complutense, Madrid) for help with the Southern experiment, Karin Lipfert (IPK, Department Cytogenetics and Genome Analysis, Gatersleben) for help with figure preparation, and Doreen Stengel (IPK, Department Cytogenetics and Genome Analysis, Gatersleben) for submitting Illumina reads. We are also grateful to Ali Banaei Moghaddam (IPK, Department Cytogenetics and Genome Analysis, Gatersleben) for help with uploading genome survey sequences, and to Ingo Schubert (IPK, Department Cytogenetics and Genome Analysis, Gatersleben) for fruitful discussions. This work was supported by the Institut für Pflanzen-genetik und Kulturpflanzenforschung (Gatersleben), the Deutsche

Forschungsgemeinschaft (SPP 1384), and by grants P501/12/G090 (Czech Science Foundation) and RVO 60077344 (Academy of Sciences of the Czech Republic) to J.M.

SUPPORTING INFORMATION

Additional Supporting Information may be found in the online version of this article.

Data S1. Assembled contigs representative of individual clusters of satellite DNA.

Figure S1. Dot-plot similarity comparison of assembled contigs representing the most abundant satellite repeats.

Figure S2. Southern analysis reveals a ladder-like pattern typical for satellite DNA.

Figure S3. Immunolabeling of *L. elegans* mitotic metaphase chromosomes.

Figure S4. Distribution of DNA methylation (5mC immunolabeling) in *L. elegans* interphase nuclei.

Figure S5. DNA replication behavior of *L. elegans*.

Table S1. Sequences of oligonucleotides used in the present study.

Table S2. Sequenced clones from a partial genomic library screened by dot-blot hybridization.

REFERENCES

- Albertson, D.G., Rose, A.M. and Villeneuve, A.M. (1997) Chromosome organization, mitosis, and meiosis. In *C. elegans* II, 2nd edn (Riddle, D.L., Blumenthal, T., Meyer, B.J. and Priess, J.R., eds). Cold Spring Harbor, NY: Cold Spring Harbor Laboratory Press, pp. 47–78.
- d'Alençon, E., Sezutsu, H., Legeai, F. et al. (2010) Extensive synteny conservation of holocentric chromosomes in Lepidoptera despite high rates of local genome rearrangements. *Proc. Natl Acad. Sci. USA*, **107**, 7680–7685.
- d'Alençon, E., Negre, N., Stanojic, S., Allassouir, B., Gimenez, S., Leger, A., Abd-Alla, A., Juliant, S. and Fournier, P. (2011) Characterization of a CENP-B homolog in the holocentric Lepidoptera *Spodoptera frugiperda*. *Gene*, **485**, 91–101.
- Barlow, P.W. and Nevin, D. (1976) Quantitative karyology of some species of *Luzula*. *Plant Syst. Evol.* **125**, 77–86.
- Bennett, M.D. and Leitch, A.R. (2010) Plant DNA C-values database. Release 5.0, December 2010 [WWW document]. URL data.kew.org/cvalues/ [accessed on 31 October 2012].
- Bernardini, J.V. and Lima-de-Faria, A. (1967) Asynchrony of DNA replication in the chromosomes of *Luzula*. *Chromosoma*, **22**, 91–100.
- Bongiorni, S., Fiorenzo, P., Pippoletti, D. and Pranter, G. (2004) Inverted meiosis and meiotic drive in mealybugs. *Chromosoma*, **112**, 331–341.
- Buchwitz, B.J., Ahmad, K., Moore, L.L., Roth, M.B. and Henikoff, S. (1999) A histone H3-like protein in *C. elegans*. *Nature*, **401**, 547–548.
- C. elegans* Sequencing Consortium (1998) Genome sequence of the nematode *C. elegans*: a platform for investigating biology. *Science*, **282**, 2012–2018.
- Clarke, L. and Carbon, J. (1985) The structure and function of yeast centromeres. *Annu. Rev. Genet.* **19**, 29–56.
- Collet, C. and Westerman, M. (1984) Interspersed distribution patterns of C-bands and satellite DNA in the holocentric chromosomes of *Luzula flaccida* (Juncaceae). *Genetica*, **63**, 175–179.
- Collet, C. and Westerman, M. (1987) Interspecies comparison of the highly repeated DNA of Australasian *Luzula* (Juncaceae). *Genetica*, **74**, 95–103.
- Costas, C., Sanchez, M.D.I.P., Sequeira-Mendes, J. and Gutierrez, C. (2011) Progress in understanding DNA replication control. *Plant Sci.* **181**, 203–209.
- Dernburg, A.F. (2001) Here, there, and everywhere: kinetochore function on holocentric chromosomes. *J. Cell Biol.* **153**, 33–38.
- Doležel, J., Greilhuber, J., Lucretti, S., Meister, A., Lysák, M.A., Nardi, L. and Obermayer, R. (1998) Plant genome size estimation by flow cytometry: inter-laboratory comparison. *Ann. Bot.* **82**, 17–26.
- Dong, F.G., Miller, J.T., Jackson, S.A., Wang, G.L., Ronald, P.C. and Jiang, J.M. (1998) Rice (*Oryza sativa*) centromeric regions consist of complex DNA. *Proc. Natl Acad. Sci. USA*, **95**, 8135–8140.
- Fuchs, J., Demidov, D., Houben, A. and Schubert, I. (2006) Chromosomal histone modification patterns – from conservation to diversity. *Trends Plant Sci.* **11**, 199–208.
- Fuchs, J., Jovtchev, G. and Schubert, I. (2008) The chromosomal distribution of histone methylation marks in gymnosperms differs from that of angiosperms. *Chromosome Res.* **16**, 891–898.
- Gassmann, R., Rechtsteiner, A., Yuen, K.W. et al. (2012) An inverse relationship to germline transcription defines centromeric chromatin in *C. elegans*. *Nature*, **484**, 534–537.
- Gerlach, W.L. and Bedbrook, J.R. (1979) Cloning and characterization of ribosomal RNA genes from wheat and barley. *Nucleic Acids Res.* **7**, 1869–1885.
- Gernand, D., Demidov, D. and Houben, A. (2003) The temporal and spatial pattern of histone H3 phosphorylation at serine 28 and serine 10 is similar in plants but differs between mono- and polycentric chromosomes. *Cytogenet. Genome Res.* **101**, 172–176.
- Guerra, M. and Garcia, M.A. (2004) Heterochromatin and rDNA sites distribution in the holocentric chromosomes of *Cuscuta approximata* Bab. (Convolvulaceae). *Genome*, **47**, 134–140.
- Guerra, M., Brasileiro-Vidal, A.C., Arana, P. and Puertas, M.J. (2006) Mitotic microtubule development and histone H3 phosphorylation in the holocentric chromosomes of *Rhynchospora tenuis* (Cyperaceae). *Genetica*, **126**, 33–41.
- Guerra, M., Cabral, G., Cuacos, M., Gonzalez-Garcia, M., Gonzalez-Sanchez, M., Vega, J. and Puertas, M.J. (2010) Neocentrics and holokinetics (holocentrics): chromosomes out of the centromeric rules. *Cytogenet. Genome Res.* **129**, 82–96.
- Haizel, T., Lim, Y.K., Leitch, A.R. and Moore, G. (2005) Molecular analysis of holocentric centromeres of *Luzula* species. *Cytogenet. Genome Res.* **109**, 134–143.
- Hall, A.E., Keith, K.C., Hall, S.E., Copenhaver, G.P. and Preuss, D. (2004) The rapidly evolving field of plant centromeres. *Curr. Opin. Plant Biol.* **7**, 108–114.
- Hawkins, J.S., Kim, H., Nason, J.D., Wing, R.A. and Wendel, J.F. (2006) Differential lineage-specific amplification of transposable elements is responsible for genome size variation in *Gossypium*. *Genome Res.* **16**, 1252–1261.
- Heckmann, S. and Houben, A. (2012) Holokinetic centromeres. In *Plant Centromere Biology*, Vol. 1 (Jiang, J. and Birchler, J., eds). Oxford: Wiley-Blackwell, in press.
- Heckmann, S., Schroeder-Reiter, E., Kumke, K., Ma, L., Nagaki, K., Murata, M., Wanner, G. and Houben, A. (2011) Holocentric chromosomes of *Luzula elegans* are characterized by a longitudinal centromere groove, chromosome bending, and a terminal nucleolus organizer region. *Cytogenet. Genome Res.* **134**, 220–228.
- Higgins, A.W., Gustashaw, K.M. and Willard, H.F. (2005) Engineered human dicentric chromosomes show centromere plasticity. *Chromosome Res.* **13**, 745–762.
- Hill, C.A., Guerrero, F.D., Van Zee, J.P., Geraci, N.S., Walling, J.G. and Stuart, J.J. (2009) The position of repetitive DNA sequence in the southern cattle tick genome permits chromosome identification. *Chromosome Res.* **17**, 77–89.
- Houben, A. and Schubert, I. (2003) DNA and proteins of plant centromeres. *Curr. Opin. Plant Biol.* **6**, 554–560.
- Houben, A., Kynast, R., Heim, U., Hermann, H., Jones, R. and Forster, J. (1996) Molecular cytogenetic characterisation of the terminal heterochromatic segment of the B-chromosome of rye (*Secale cereale*). *Chromosoma*, **105**, 97–103.
- Houben, A., Demidov, D., Gernand, D., Meister, A., Leach, C.R. and Schubert, I. (2003) Methylation of histone H3 in euchromatin of plant chromosomes depends on basic nuclear DNA content. *Plant J.* **33**, 967–973.
- Houben, A., Demidov, D., Caperta, A.D., Karimi, R., Agueci, F. and Vlasenko, L. (2007a) Phosphorylation of histone H3 in plants – a dynamic affair. *Biochim. Biophys. Acta*, **1769**, 308–315.
- Houben, A., Schroeder-Reiter, E., Nagaki, K., Nasuda, S., Wanner, G., Murata, M. and Endo, T. (2007b) CENH3 interacts with the centromeric retrotransposon *cereba* and GC-rich satellites and locates to centromeric substructures in barley. *Chromosoma*, **116**, 275–283.

- Howe, M., McDonald, K.L., Albertson, D.G. and Meyer, B.J. (2001) HIM-10 is required for kinetochore structure and function on *Caenorhabditis elegans* holocentric chromosomes. *J. Cell Biol.* **153**, 1227–1238.
- Kalitsis, P. and Choo, K.H. (2012) The evolutionary life cycle of the resilient centromere. *Chromosoma*, **121**, 327–340.
- Kato, A., Albert, P.S., Vega, J.M. and Birchler, J.A. (2006) Sensitive fluorescence *in situ* hybridization signal detection in maize using directly labeled probes produced by high concentration DNA polymerase nick translation. *Biotech. Histochem.* **81**, 71–78.
- Lamb, J.C., Yu, W.C., Han, F.P. and Birchler, J.A. (2007) Plant chromosomes from end to end: telomeres, heterochromatin and centromeres. *Curr. Opin. Plant Biol.* **10**, 116–122.
- Liu, T., Rechtsteiner, A., Egelhofer, T.A. *et al.* (2011) Broad chromosomal domains of histone modification patterns in *C. elegans*. *Genome Res.* **21**, 227–236.
- Macas, J., Meszaros, T. and Nouzova, M. (2002) PlantSat: a specialized database for plant satellite repeats. *Bioinformatics*, **18**, 28–35.
- Macas, J., Neumann, P. and Navratilova, A. (2007) Repetitive DNA in the pea (*Pisum sativum* L.) genome: comprehensive characterization using 454 sequencing and comparison to soybean and *Medicago truncatula*. *BMC Genomics*, **8**, 427.
- Macas, J., Neumann, P., Novak, P. and Jiang, J. (2010) Global sequence characterization of rice centromeric satellite based on oligomer frequency analysis in large-scale sequencing data. *Bioinformatics*, **26**, 2101–2108.
- Macas, J., Kejnovsky, E., Neumann, P., Novak, P., Koblizkova, A. and Vyskot, B. (2011) Next generation sequencing-based analysis of repetitive DNA in the model dioecious plant *Silene latifolia*. *PLoS ONE*, **6**, e27335.
- Maddox, P.S., Oegema, K., Desai, A. and Cheeseman, I.M. (2004) “Holo”er than thou: chromosome segregation and kinetochore function in *C. elegans*. *Chromosome Res.* **12**, 641–653.
- Maniatis, T., Fritsch, E.F. and Sambrook, J. (1982) *Molecular Cloning: A Laboratory Manual*. Cold Spring Harbor, NY: Cold Spring Harbor Laboratory.
- Marques, A., Fuchs, J., Ma, L., Heckmann, S., Guerra, M. and Houben, A. (2011) Characterization of eu- and heterochromatin of citrus with a focus on the condensation behavior of 45S rDNA chromatin. *Cytogenet. Genome Res.* **134**, 72–82.
- Melters, D.P., Paliulis, L.V., Korf, I.F. and Chan, S.W. (2012) Holocentric chromosomes: convergent evolution, meiotic adaptations, and genomic analysis. *Chromosome Res.* **20**, 579–593.
- Mola, L.M. and Papeschi, A.G. (2006) Holokinetic chromosomes at a glance. *J. Basic Appl. Genet.* **17**, 17–33.
- Nagaki, K., Kashiwara, K. and Murata, M. (2005) Visualization of diffuse centromeres with centromere-specific histone H3 in the holocentric plant *Luzula nivea*. *Plant Cell*, **17**, 1886–1893.
- Neumann, P., Navratilova, A., Koblizkova, A., Kejnovsky, E., Hribova, E., Hobza, R., Widmer, A., Dolezel, J. and Macas, J. (2011) Plant centromeric retrotransposons: a structural and cytogenetic perspective. *Mob. DNA*, **2**, 4.
- Neumann, P., Navratilova, A., Schroeder-Reiter, E., Koblizkova, A., Steinbauerova, V., Chocholova, E., Novak, P., Wanner, G. and Macas, J. (2012) Stretching the rules: monocentric chromosomes with multiple centromere domains. *PLoS Genet.* **8**, e1002777.
- Nonomura, K.I. and Kurata, N. (2001) The centromere composition of multiple repetitive sequences on rice chromosome 5. *Chromosoma*, **110**, 284–291.
- Nordenskiöld, H. (1962) Studies of meiosis in *Luzula purpurea*. *Hereditas*, **48**, 503–519.
- Novak, P., Neumann, P. and Macas, J. (2010) Graph-based clustering and characterization of repetitive sequences in next-generation sequencing data. *BMC Bioinformatics*, **11**, 378.
- Ray, J.H. and Venkateswaran, S. (1978) Constitutive heterochromatin distribution in monocentric and polycentric chromosomes. *Chromosoma*, **66**, 341–350.
- Ray, J.M. and Venkateswaran, S. (1979) DNA replication, ³H-cRNA *in situ* hybridization and C-band patterns in the polycentric chromosomes of *Luzula purpurea* Link. *Chromosoma*, **74**, 337–346.
- Schmidt, T. and Heslop-Harrison, J.S. (1998) Genomes, genes and junk: the large-scale organization of plant chromosomes. *Trends Plant Sci.* **3**, 195–199.
- Schulte, D., Ariyadasa, R., Shi, B.J. *et al.* (2011) BAC library resources for map-based cloning and physical map construction in barley (*Hordeum vulgare* L.). *BMC Genomics*, **12**, 247.
- Sheikh, S.A. and Kondo, K. (1995) Differential staining with orcein, giemsa, CMA, and DAPI for comparative chromosome study of 12 species of Australian *Drosera* (Droseraceae). *Am. J. Bot.* **82**, 1278–1286.
- Spence, J.M., Blackman, R.L., Testa, J.M. and Ready, P.D. (1998) A 169-base pair tandem repeat DNA marker for subtelomeric heterochromatin and chromosomal rearrangements in aphids of the *Myzus persicae* group. *Chromosome Res.* **6**, 167–175.
- Stein, L.D., Bao, Z., Blasiar, D. *et al.* (2003) The genome sequence of *Caenorhabditis briggsae*: a platform for comparative genomics. *PLoS Biol.* **1**, e45.
- Tartarotti, E. and de Azeredo-Oliveira, M.T.V. (1999) Heterochromatin patterns in triatomines of the genus *Panstrongylus*. *Cytobios*, **99**, 113–122.
- Tenaillon, M.I., Hufford, M.B., Gaut, B.S. and Ross-Ibarra, J. (2011) Genome size and transposable element content as determined by high-throughput sequencing in maize and *Zea luxurians*. *Genome Biol. Evol.* **3**, 219–229.
- Vanzela, A.L.L. and Guerra, M. (2000) Heterochromatin differentiation in holocentric chromosomes of *Rhynchospora* (Cyperaceae). *Genet. Mol. Biol.* **23**, 453–456.
- Xia, Q.Y., Wang, J., Zhou, Z.Y. *et al.* (2008) The genome of a lepidopteran model insect, the silkworm *Bombyx mori*. *Insect Biochem. Mol. Biol.* **38**, 1036–1045.
- Zhang, W., Friebe, B., Gill, B.S. and Jiang, J. (2010) Centromere inactivation and epigenetic modifications of a plant chromosome with three functional centromeres. *Chromosoma*, **119**, 553–563.
- Zinkowski, R.P., Meyne, J. and Brinkley, B.R. (1991) The centromere-kinetochore complex: a repeat subunit model. *J. Cell Biol.* **113**, 1091–1110.